

On the Gouy-Chapman-Stern model of the electrical double-layer structure with a generalized Boltzmann factor

Anis Allagui^{a,b,c,*}, Hachemi Benaoum^e, Oleg Olendski

^a*Dept. of Sustainable and Renewable Energy Engineering, University of Sharjah, Sharjah, UAE*

^b*Center for Advanced Materials Research, Research Institute of Sciences and Engineering, University of Sharjah, Sharjah, UAE*

^c*Dept. of Mechanical and Materials Engineering, Florida International University, Miami, FL33174, United States*

^d*Dept. of Applied Physics and Astronomy, University of Sharjah, PO Box 27272, Sharjah, United Arab Emirates*

^e*Dept. of Applied Physics and Astronomy, University of Sharjah, PO Box 27272, Sharjah, United Arab Emirates*

Abstract

The classical treatment of the electrical double-layer (EDL) structure at a planar metal/electrolyte junction via the Gouy-Chapman-Stern (GCS) approach is based on the Poisson equation relating the electrostatic potential to the net mean charge density. The ions concentration in the diffuse layer are assumed to follow the Boltzmann distribution law, i.e. $\propto \exp(-\tilde{\psi})$ where $\tilde{\psi}$ is the dimensionless electrostatic potential. However, even in stationary equilibrium in which variables are averaged over a large number of elementary stochastic events, deviations from the mean-value are expected. In this study we evaluate the behavior of the EDL by assuming some small perturbations superposed on top of its Boltzmann distribution of ion concentrations using the Tsallis nonextensive statistics framework. With this we assume the ion concentrations to be proportional to $[1 - (1 - q)\tilde{\psi}]^{1/(1-q)} = \exp_q(-\tilde{\psi})$ with q being a real parameter that characterizes the system's statistics. We derive analytical expression and provide computational results for the overall differential capacitance of the EDL structure, which, depending on the values of the parameter q can show both the traditional inverse bell-shaped curves for aqueous solutions and bell curves observed with ionic liquids.

Keywords: Double-layer capacitor, Tsallis distribution, Boltzmann distribution, Capacitance

1. Introduction

The electrical double-layer (EDL) is more than a century-old fundamental topic of electrochemistry and physical chemistry [1–5]. It is found in many applications such as in membrane science and technology [6, 7], water desalination by capacitive ion removal [5, 8, 9], capacitive mixing [10–12], energy storage in porous electrodes and fractional-order capacitors [4, 13–17], colloidal suspensions [18, 19], etc. It refers to the general phenomenon of charge separation across an interfacial surface, which can be imagined as a plane that separates two adjacent and distinct phases (e.g. metal and electrolyte) having excess electronic or ionic charges (see Fig. 1). At such an electrified interface, the electrode charge is not necessarily constant, but on the contrary fluctuates in response to the stochastic

*Corresponding author

Email address: aallagui@sharjah.ac.ae (Anis Allagui)

thermal motions in the adjacent electrolyte. These fluctuations are related to a set of configuration variables including the number, positions and momenta of mobile ions of each species near the electrode, and become important as the correlation between species increases [20, 21]. The extent of these correlations is related to the nature of the interfacial liquid, and is expected to increase with the increase of ions concentration as well as in nanometer-sized confined geometries at the electrode surface. As a result the electrical properties of within small scales of the electrode, such as the differential capacitance, electrostatic potential or accumulated charge density for instance, are expected to be affected by the statistics of these microscopic fluctuations [21, 22].

Several computational models such as Monte-Carlo (MC), molecular dynamics (MD) and density functional theory (DFT) simulations are now very apt to provide good descriptions of the EDL structure [9, 12, 22, 23]. However, because of the computational resources needed for the explicit microscopic analysis of large numbers of interacting solvent and mobile ions, mean-field calculations remain popular due their simplicity and comparatively good accuracy [4, 5, 13]. The classical Gouy-Chapman-Stern (GCS) approach in which the Poisson-Boltzmann (PB) equations are used for the treatment of the diffuse part of the solvent (reviewed in Sect. 1) is widely used because it is verified to be asymptotically correct in the weak-coupling regime and it provides the essential of the EDL properties [1, 2, 5, 7, 24–26]. It assumes the equilibrium ion concentrations to decay exponentially with the distance from the interface following a Boltzmann distribution function with respect to the mean electrostatic potential energy in the EDL. This statistical representation is considered and widely used as the generic case for thermal equilibrium of many uncorrelated or weakly-correlated systems. However, when effects such as ion-ion correlations, ion polarizability, finite size of ions, electrostriction and dielectric saturation of the solvent cannot be ignored, the GCS model becomes less reliable in describing the features of the EDL [2, 20, 27]. Furthermore, if the electrode surface is fractal and/or consisting of small confined geometries, the stochastic nature of state variables associated with the mobile ions for instance is also expected to deviate from Boltzmann’s distribution profile [28].

The purpose of this study is to incorporate into the mean-field GCS model the Tsallis q -deformed exponential distribution [28–34] for the ion concentrations in the interfacial liquid (Sect. 2). The same analysis can be applied in principle to other approaches dealing with the EDL structure. The q -exponential function we are considering allows the presence of random fluctuations of ion concentrations around their mean values, which in turn provides a sort of a generalized Boltzmann factor. With this approach, one can still analyze a microscopic system in which correlations are expected as if they were absent [28]. We provide analytical solutions for the charge density and differential capacitance from the boundary-value PB problem parameterized with the value of q that can be attributed to the strength of elementary noise sources in the EDL structure. A similar approach that came to our attention during the writing of this paper was reported by Garcia-Morales et al. [28], in which the focus was mainly on the q -dependence of the PB equation for describing counterion concentration around a charged surface. However, this study is further concerned with the overall capacitive performance of the EDL structure by taking into account the series combination of the Helmholtz capacitance and the diffuse layer capacitance for a symmetric electrolyte, which was not provided in ref. [28]. We also evaluate the effect of the values of q (taken between -1 to 1) on the EDL capacitance vs. voltage

profiles which allowed to capture both the traditional inverse bell-shaped curves for aqueous solutions and bell-like curves measured for ionic liquids.

2. The Gouy-Chapman-Stern Model

The standard model to describe the equilibrium EDL structure at the junction metal/electrolyte (dilute solutions) is the GCS mean-field model which can quantitatively explain most experimental results. It consists of subdividing the EDL into (i) a first sheet of uniform constant electronic charges on the metal surface, (ii) a charge-free inner compact layer or Helmholtz layer (also known as Stern layer) of a few angstrom in width and constant charge, and (iii) an outer, semi-infinite diffuse layer (also known as Gouy-Chapman layer) that extends into the bulk electrolyte and contains anions and cations of a certain distribution [24] (see Fig. 1). Ions are assumed to be ideal point charges in local thermodynamic equilibrium within an isolated planar interface, and the solvent is assumed to be a dielectric continuum [8]. There are many subsequent modified and refined versions of the GCS model that apply for instance corrections for ion crowding or dielectric saturation [35–37], but here we use the simplest treatment for one electrode only that captures good enough the essentials. Only physical adsorption in the diffuse layer is considered to compensate the electronic charges, but no Faradaic charge-transfer reactions and/or ion adsorption are taken into account.

In the diffuse layer part of the GCS's model, the electrolyte is treated using the mean-field PB model. For dilute solutions with negligible correlations, the ions' concentrations at a perpendicular distance $x \geq 0$ from a large lateral surface area metal electrode (one-dimensional problem in which the edge effects are ignored) are assumed to be related to the mean electrostatic potential ψ_x by the continuous Boltzmann distribution function:

$$C_{x_i} = C_{x_i}^0 \exp\left(-\frac{z_i F \psi_x}{RT}\right) \quad (1)$$

where $C_{x_i}^0$ and z_i are the average ion concentration (for $\psi_x = 0$) and charge number of species i (cation and anion), respectively. The term $RT/F = k_B T/e$ (with R the ideal gas constant, F the Faraday's constant, k_B the Boltzmann's constant, e the elemental electronic charge, and T the absolute temperature) is the thermal voltage. The molar electrical interaction energy in the Boltzmann factor takes into account the term $z_i F \psi_x$ only, and other contributions are ignored in this study. The approximation of C_{x_i} by a Boltzmann distribution is a standard tool used to evaluate many other thermodynamic properties of systems, but is valid for some ideal conditions only, i.e. elastic collision between particles, particles are identical and independent of one another, etc. It assumes that the ratio of equilibrium ionic concentrations at two locations x_i and x_j in the solution, i.e. C_{x_i}/C_{x_j} , at which the mean electrostatic potentials are ψ_{x_i} and ψ_{x_j} , respectively, is related to the work needed to carry an ion of charge ze from x_i to x_j , i.e. $-ze(\psi_{x_i} - \psi_{x_j})$, through the exponential Boltzmann factor given in Eq. 1 [38].

Now the distribution of the mean electrostatic potential ψ_x in Eq. 1 is governed by the Poisson equation that connects the net volume charge density ρ_x at the distance x from the interface with the corresponding potential ψ_x as:

$$\frac{d^2 \psi_x}{dx^2} = -\frac{\rho_x}{\epsilon} \quad (2)$$

where ϵ is the uniform dielectric permittivity of the solvent in units of the vacuum dielectric constant ϵ_0 . The mean charge density ρ_x can be expressed as the sum $\rho_x = \sum_i z_i F C_{x_i}$ over the ions species, which leads to the second-order nonlinear differential equation:

$$\frac{d^2\psi_x}{dx^2} = -\frac{1}{\epsilon} \sum_i z_i F C_{x_i}^0 \exp\left(-\frac{z_i F \psi_x}{RT}\right) \quad (3)$$

With the change of variables $p = d\psi_x/dx$, such that $d^2\psi_x/dx^2 = dp/dx = p dp/d\psi_x$, we rewrite Eq. 3 as:

$$\frac{1}{2} \left(\frac{d\psi_x}{dx}\right)^2 = \frac{RT}{\epsilon} \sum_i C_{x_i}^0 \left[\exp\left(\frac{-z_i F \psi_x}{RT}\right) \right] + B \quad (4)$$

The integration constant B is determined using the boundary conditions $\psi_x(x \rightarrow \infty) = 0$ (electroneutrality) and $d\psi_x/dx = 0$ (electrostatic field must vanish at the mid-plane) so that:

$$\left(\frac{d\psi_x}{dx}\right)^2 = \frac{2RT}{\epsilon} \sum_i C_{x_i}^0 \left[\exp\left(\frac{-z_i F \psi_x}{RT}\right) - 1 \right] \quad (5)$$

If we consider the special case of a symmetric electrolyte (i.e. two ionic species; one positively charged and one negatively charged with $|z_i| = z$ and $C_{x_i}^0 = C_x^0, \forall i$), we obtain the analytical solution of GCS model for a positively charged electrode as:

$$\frac{d\psi_x}{dx} = -\sqrt{\frac{8RT C_x^0}{\epsilon}} \sinh\left(\frac{zF\psi_x}{2RT}\right) < 0 \quad (6)$$

in which physical arguments impose that the appropriate sign should be as shown. Note that Eq. 6 can be written in the dimensionless form $d(\tilde{\psi}_x/2)/d\tilde{x} = -\sinh(\tilde{\psi}_x/2)$, where $\tilde{\psi}_x = \psi/(RT/zF)$ and $\tilde{x} = x/\lambda_D$ with $\lambda_D = \sqrt{\epsilon RT/2z^2 F^2 C_x^0}$ being the Debye screening length for the symmetric electrolyte. It can also be linearized in the limit of low potentials leading to the Debye-Hückel model. With Eq. 6 one can obtain the total net charge per unit surface Q_x within the diffuse layer as:

$$\left(\frac{d\psi_x}{dx}\right)_{x=d} = -\frac{1}{\epsilon} \int_{x=d}^{\infty} \rho_x dx = -\frac{Q_x}{\epsilon} \quad (7)$$

Combining Eq. 6 and Eq. 7 gives the total net charge within the diffuse layer as:

$$Q_x = \sqrt{8\epsilon RT C_x^0} \sinh\left(\frac{zF\psi_d}{2RT}\right) \quad (8)$$

To determine the specific capacitance of the diffuse layer, the net charge (Eq. 8) is differentiated with respect to the potential, which gives the well-known nonlinear expression:

$$C_{\text{diff}} = \sqrt{\frac{2\epsilon z^2 F^2 C_x^0}{RT}} \cosh\left(\frac{zF\psi_d}{2RT}\right) \quad (9)$$

that depends on both the potential ψ_d and the properties of the electrolyte C_x^0 and ϵ . The expression for C_{diff} can also be expressed in a dimensionless form as $\tilde{C}_{\text{diff}} = \lambda_D C_{\text{diff}}/\epsilon = \cosh(\tilde{\psi}_x/2)$ [4]. The overall EDL capacitance of the electrode is then computed from the combination in series of the two capacitances arising from the Helmholtz inner layer (of constant capacitance $C_H = \epsilon/4\pi d$ with d being its thickness) and the diffuse layer, such that:

$$C_{\text{dl}}^{-1} = C_H^{-1} + C_{\text{diff}}^{-1} \quad (10)$$

A plot of C_{dl} vs. potential ($\psi_d > 0$) for different values of the bulk concentrations C_x^0 is shown in Fig. 2. We took the values of $C_{\text{H}} = 28 \mu\text{F cm}^{-2}$, $\epsilon = 80 \epsilon_0$, $z = 1$, and $T = 298 \text{ K}$. At large voltages and for concentrated electrolytes, the overall capacitance is determined by that of the Helmholtz layer, independently of the ion concentrations, whereas as the voltage is decreased and for very dilute electrolytes, the contribution of the diffuse layer becomes more important. For $\psi_d = 0$, we have the reciprocal of the overall capacitance $C_{\text{dl}}^{-1} = C_{\text{H}}^{-1} + (2\epsilon z^2 F^2 C_x^0 / RT)^{-0.5}$.

3. The Generalized Boltzmann Factor

The Boltzmann distribution function, as mentioned above, provides a valid approximation only under certain assumptions for equilibrium thermodynamic [25, 39, 40]. While it allows a relatively accurate description of macroscopic systems in which a very large number of stochastic events take place, when one goes to smaller scales for instance, such a description breaks down [41]. It is expected that at small dimensions, fluctuations of some intensive quantity such as temperature or pressure or chemical potential for example with respect to that of the surrounding reservoir, and contributions from the surface energy would play crucial roles in determining the state of the system under consideration [42]. The system in this case is in stationary quasi-thermodynamic equilibrium with the reservoir. This situation is closely related to the case of the EDL structure within small sizes in the nanopores of porous electrodes. The effects of fluctuations and long-range interactions are actually more prominent at this level where the number of particles can be much smaller than Avogadro's number.

Moy et al. [7] have confirmed that some physical quantities, such as the force on a test ion, computed using the PB approximation deviates from the predictions with those of Brownian dynamics simulations (using the Langevin equation) in which individual ions are treated explicitly. The difference widens as the distance of the ion from the channel is lower than the Debye's length. The same discrepancies on the conductance and concentration profiles in cylindrical channels and a potassium channel were reported between the Poisson–Nernst–Planck theory (commonly used for non-equilibrium ion transport problems) vs. the Brownian dynamics [26]. In another study by Härtel et al. [9], DFT and MD simulations were applied to the EDL structure and showed very good agreement for the ions concentration profiles, but clear deviations from those computed with the PB theory are observed.

Motivated by these observations, the purpose of this study is to evaluate the behavior of the EDL structure using a more general Boltzmann factor as proposed by Tsallis [31], and later extended by Beck and Cohen [32–34] and others (see ref. [29] and references within). These statistical mechanics approaches have been introduced as a way to systematically describe complex statistical systems that behave like the superposition of many Boltzmann distributions, which makes the single Boltzmann distribution to be nothing but a special limiting case. Such systems usually involve long-range interactions, non-Markovian memory effects and anomalous diffusion; examples and applications can be found in different disciplines of science and engineering [43, 44]. At the microscopic level, systems relax toward thermodynamic equilibrium (or more appropriately stationary nonequilibrium [45]) following a single exponential decay, type Boltzmann, i.e. the probability of finding the system at some specific state of energy ϵ is proportional to $\exp(-\beta\epsilon)$

where β is a local inverse temperature. At a larger scale, the local variable β (other variables can be considered) is not well-defined and experiences fluctuations following a certain probability distribution function $f(\beta)$, which depends on the underlying dynamics of the system and is a priori unknown [45]. From Beck and Cohen [32], the generalized Boltzmann factor can be written as the integral over all possible fluctuating inverse temperatures β as:

$$B(E) = \int_0^{\infty} f(\beta) \exp(-\beta E) d\beta \quad (11)$$

For most physical systems a distribution where the random variable β is nonnegative is needed. In particular, if $f(\beta)$ is assumed to follow a gamma probability distribution function which arises naturally for a fluctuating environment with a finite number of degrees of freedom, such that:

$$f(\beta) = \frac{1}{b\Gamma(c)} (\beta/b)^{c-1} \exp(-\beta/b) \quad (12)$$

where c and b are positive parameters, Eq. 11 leads to the generalized Boltzmann factor in Tsallis statistics [29, 31, 32, 40, 44, 46]:

$$B(E) = (1 + bE)^{-c} = [1 - (1 - q)\beta_0 E]^{1/(1-q)} = \exp_q(-\beta_0 E) \quad (13)$$

with $1/(q - 1) = c$, $\beta_0 = \int_0^{\infty} \beta f(\beta) d\beta = bc$ is the average of the fluctuating β , and $\exp_q(y)$ denotes the q -exponential function. The parameter q is a real number that characterizes the system's statistics, and is defined by the ratio of standard variation and mean of the distribution $f(\beta)$ ($q = 1$ if there are no fluctuations) [32]. Note that (i) for $q < 1$, $\exp_q(y) = 0$ for $y < -1/(1 - q)$ and $\exp_q(y) = [1 + (1 - q)y]^{1/(1-q)}$ for $y \geq -1/(1 - q)$, (ii) for $q = 1$, $\exp_q(y) = \exp(y)$ for $\forall y$, and (iii) for $q > 1$, $\exp_q(y) = [1 + (1 - q)y]^{1/(1-q)}$ for $y < 1/(q - 1)$ [44].

4. The Extended Gouy-Chapman-Stern Model

By applying generically the generalized Boltzmann factor given by Eq. 13 to the concentrations of charged ions in the EDL structure (instead of Eq. 1), we write the q -exponential relation [30]:

$$C_{x_i}^q = C_{x_i}^0 \exp_q\left(-\frac{z_i F \psi_x}{RT}\right) \quad (14)$$

Again, this means that the fluctuations of the mean-field value of the ion concentrations are assumed to follow a gamma distribution with the parameter $q = 1 + 1/c$ representing the extent of these fluctuations. The adequate determination of the statistical distribution of such ions concentration is very difficult to obtain. If $q = 1$, the traditional Boltzmann factor given in Eq. 1 is immediately recovered from Eq. 14. Plots of $C_{x_i}^q$ as a function of potential ψ_x for different values of $q \leq 1$ are shown in Fig. 3. In a semi-logarithmic scale, it is only the Boltzmann distribution that would result in a straight line with slope $-zF/RT \ln(10)$. Otherwise, Decreasing the value of q from unity implies steeper decrease of the ionic concentration following a power-law profile as shown in the figure. This means that contrary to the exponential decay in which subsystems are uncorrelated, values of q different from one implies some form of internal correlations between subsystems.

The q -modified PB model becomes then:

$$d\left(\frac{d\psi_x}{dx}\right)^2 = -\frac{2F}{\epsilon} \sum_i C_{x_i}^0 z_i \exp_q\left(-\frac{z_i F \psi_x}{RT}\right) d\psi_x \quad (15)$$

which leads after integration to:

$$\begin{aligned} \left(\frac{d\psi_x}{dx}\right)^2 &= \frac{2RT}{\epsilon(2-q)} \times \\ &\sum_i C_{x_i}^0 \left[\left(1 - (1-q) \frac{z_i F \psi_x}{RT}\right) \exp_q\left(-\frac{z_i F \psi_x}{RT}\right) - 1 \right] \end{aligned} \quad (16)$$

We verify that for $q = 1$, Eq. 16 readily simplifies to the expression given in Eq. 5. For the case of a symmetric 1:1 electrolyte, we obtain:

$$\begin{aligned} \left(\frac{d\psi_x}{dx}\right)^2 &= \frac{4RTC_x^0}{\epsilon(2-q)} \times \\ &\left[\cosh_q\left(\frac{zF\psi_x}{RT}\right) + (1-q) \left(\frac{zF\psi_x}{RT}\right) \sinh_q\left(\frac{zF\psi_x}{RT}\right) - 1 \right] \end{aligned} \quad (17)$$

where the q -hyperbolic functions \cosh_q and \sinh_q are defined respectively as [47]:

$$2 \cosh_q(y) = \exp_q(y) + \exp_q(-y) \quad (18a)$$

$$2 \sinh_q(y) = \exp_q(y) - \exp_q(-y) \quad (18b)$$

Now using the q -identities:

$$\cosh_q(y) = 2 \sinh_{2q-1}^2(y/2) + \exp_{2q-1}\left[-(1-q)y^2/2\right] \quad (19a)$$

$$\sinh_q(y) = 2 \sinh_{2q-1}(y/2) \cosh_{2q-1}(y/2) \quad (19b)$$

we obtain the following expression for the electric field:

$$\frac{d\psi_x}{dx} = -\sqrt{\frac{8RTC_x^0}{\epsilon(2-q)}} \sinh_{2q-1}\left(\frac{zF\psi_x}{2RT}\right) h_q\left(\frac{zF\psi_x}{RT}\right) \quad (20)$$

where the function $h_q(y)$ is given by:

$$h_q(y) = \left[1 + (1-q)y \coth_{2q-1}\left(\frac{y}{2}\right) - \frac{1 - \exp_{2q-1}\left(-\frac{(1-q)y^2}{2}\right)}{2 \sinh_{2q-1}^2\left(\frac{y}{2}\right)} \right]^{0.5} \quad (21)$$

It is clear that when $q \rightarrow 1$, the classical relation given by Eq. 6 for the electric field is immediately recovered. We can write Eq. 20 in a dimensionless form as $d(\tilde{\psi}_x/2)/d\tilde{x}_q = -\sinh_{2q-1}(\tilde{\psi}_x/2)h(\tilde{\psi}_x)$ where \tilde{x}_q is the normalized dimension x with respect to a modified Debye length, $\lambda_D^q = \lambda_D \sqrt{2-q}$, which depends on the properties of the liquid as well as the extent of the fluctuations through the parameter q . λ_D^q is larger than λ_D for $q < 1$ which implies that the

scale over which the electrolyte screens the surface charge is larger with the presence of fluctuations. Finally, the q -parameterized net charge Q_x^q in the diffuse layer using the generalized Boltzmann factor is found as:

$$Q_x^q = \sqrt{\frac{8\epsilon RT C_x^0}{2-q}} \sinh_{2q-1} \left(\frac{zF\psi_d}{2RT} \right) h_q \left(\frac{zF\psi_d}{RT} \right) \quad (22)$$

and its associated diffuse capacitance is found numerically from $C_{\text{diff}}^q = \partial Q_x^q / \partial \psi_x$. The overall EDL capacitance C_{dl}^q is then computed as per Eq. 10, i.e.:

$$(C_{\text{dl}}^q)^{-1} = C_{\text{H}}^{-1} + (C_{\text{diff}}^q)^{-1} \quad (23)$$

The total charge Q_{dl}^q is obtained from the voltage integral of C_{dl}^q . Plots of $C_{\text{dl}}^q(\psi_x)$ for different values of q for a constant bulk concentration of $C_x^0 = 10^{-3} \text{ mol L}^{-1}$, are shown in Fig. 4. The capacitance at negative voltages exactly duplicate the capacitance at positive voltages shown in the figure.

5. Discussion

From Fig. 4, it is evident that incorporating the generalized Boltzmann factor for the ions concentrations into the mean-field GCS model affects greatly the capacitive performance of the EDL structure. It is understood that other electrical characteristics are also impacted, but the focus of the discussion here is on the differential EDL capacitance, and thus energy storage applications. The strength of the fluctuations increases as the value of q deviates further from unity at which the traditional Boltzmann factor is recovered. In other words, when the parameter q is less than one, it implies that there are some forms of hidden correlations within the stationary system in quasi-thermodynamic equilibrium, which means that its constituting subsystems are not statistically independent anymore as it is the case in Boltzmann theory [45]. In practice, however, the determination of an experimental value for q and the particular form of correlations between the dynamic subsystems is not trivial as mentioned above.

Fig. 4 shows also that the overall capacitance exhibits a local minimum at the origin for different values of $q > 0$, and an asymptotic increase towards the value of $C_{\text{H}} = 28 \mu\text{F cm}^{-2}$ at higher polarization. Otherwise, between these two limiting cases, the shapes of the profiles for $0 < q < 1$ are in concordance with the shapes obtained with the traditional GCS model for which $q = 1$ (compare with Fig. 2). Now because of the interdependence of internal subsystems for $q < 1$, this results is an extra contribution to the amount of entropy of the system, i.e. the entropy $S_q(A + B) \geq S_q(A) + S_q(B)$ of two subsystems A and B [40]. This non-additivity of entropy is the basis of a non-extensive Tsallis statistics. Tsallis proposed the generalized entropy $S_q = -k \sum_i p_i^q \ln_q(p_i)$ [31, 40, 44, 46], where k is a positive constant, $q \neq 1$, and the quantities $p_i = p(E_i)$ represent the probabilities for the occurrence of the i^{th} microstate and satisfy $\sum_i p_i = 1$. The function $\ln_q(y) = (y^{1-q} - 1)/(1 - q)$ denotes the q -logarithm, inverse of the q -exponential (i.e. $\ln_q[\exp_q(y)] = \exp_q[\ln_q(y)] = y$) [40]. In the limit of $q \rightarrow 1$, one recovers the classical form of Boltzmann-Gibbs entropy $S_1 = -k_B \sum_i p_i \ln(p_i)$ where $k = k_B$ is the Boltzmann constant [31]. Such additional amount of entropy, which is related to the value of q , affects negatively the net density of charge in the diffuse layer of the EDL

structure compared to the traditional case when $q = 1$. This in turn lowers the overall EDL capacitance as depicted in Fig. 4.

What is also remarkable from these results is the bell-shaped-like trend of the total capacitance when q takes values less than zero. A similar profile is observed for metal/ionic liquid double layer capacitance which exhibit a local maximum at the point of zero charge [37]. In Fig. 4, we show the example for $q = -1$ which is typical for all negative values of q . The capacitance shows a peaking value and reverse of curvature close to the origin at $\psi_x = 0$, and the same is observed when the capacitance is plotted vs. charge. It is well known that the non-linear PB theory of points ions is unable to display a change of curvature observed experimentally in ionic liquids or highly concentrated electrolytes. This change of curvature can be, nonetheless, predicted in the so-called primitive model (in which solvent effects are considered implicitly) by including ion correlations and ionic excluded volume effects. This has been shown by numerous DFT and integral equations calculations, as well as Monte Carlo, and Brownian dynamics and molecular dynamics simulations. The change of curvature of the differential capacity can be also observed in more detailed atomistic models in which solvent particles are taken into account explicitly.

Finally, the authors recognize that the main limitation of this theoretical description is the lack of a proper physical meaning for the parameter q in terms of a microscopic model. The analysis presented here is unable to provide an effective description of ion correlations (i.e., the Coulombic attraction of charged particles of opposite valence and the Coulombic repulsion of charged particles with the same valence) and ionic excluded volume effects (i.e., the fact that two ions cannot overlap due to its finite size), but this is the subject of ongoing investigations. A measurable atomistic model supporting the physical reality of the parameter q will follow to validate the use of non-extensive Tsallis statistics in EDL systems. In this sense, the parameter q can be viewed as mathematically well-fit to capture the change of curvature of the differential capacity, as it is the case for instance of fractional integro-differential equations for capturing anomalous time-domain and frequency-domain features in several physicochemical systems [16, 48–50].

6. Conclusion

In this paper, we analyzed the effect of superposing fluctuations onto the mean-value Boltzmann distribution of ion concentrations in the GCS model on the capacitive properties of the EDL structure. This was done via the q -exponential function which allows to embrace a spectrum of empirical processes connected to the degree of fluctuations in the intensive inverse temperature parameter. This compact and efficient approach provides an extended version to the classical GCS model specifically for the description of the EDL at scales in which correlation between subsystem are possible. The analytical expression for the EDL capacitance as a function of voltage and ion concentration, and parameterized with the index $q < 1$, predicts lower values than its GCS counterpart (i.e. for $q = 1$) which has been explained by super-additive entropy feature in Tsallis statics. Additionally, for values of q less than zero, the model reverses the general trend of capacitance at a metal/electrolyte junction towards that of a bell-shaped-like

profiles which are observed in ionic liquid EDL structure. Further investigations in this direction with comparison with atomistic models are being developed for future contributions.

Acknowledgement

We thank Mathijs Janssen for useful discussions and comments on an earlier version of the manuscript.

References

References

- [1] P. Delahay, Double layer and electrode kinetics, John Wiley & Sons Inc, 1965.
- [2] S. L. Carnie, G. M. Torrie, The Statistical Mechanics of the Electrical Double Layer, vol. 58, chap. 2, John Wiley & Sons, Ltd, 141–253, doi:10.1002/9780470142806.ch2, 1984.
- [3] R. Parsons, The electrical double layer: recent experimental and theoretical developments, Chemical Reviews 90 (5) (1990) 813–826.
- [4] M. Z. Bazant, K. Thornton, A. Ajdari, Diffuse-charge dynamics in electrochemical systems, Phys. Rev. E 70 (2) (2004) 021506.
- [5] P. Biesheuvel, J. Dykstra, Physics of Electrochemical Processes, www.physicsofelectrochemicalprocesses.com, 2020.
- [6] S. McLaughlin, The electrostatic properties of membranes, Annu. Rev. Biophys. Biophys. Chem. 18 (1) (1989) 113–136.
- [7] G. Moy, B. Corry, S. Kuyucak, S.-H. Chung, Tests of continuum theories as models of ion channels. I. Poisson- Boltzmann theory versus Brownian dynamics, Biophys. J. 78 (5) (2000) 2349–2363.
- [8] P. Biesheuvel, M. Bazant, Nonlinear dynamics of capacitive charging and desalination by porous electrodes, Phys. Rev. E 81 (3) (2010) 031502.
- [9] A. Härtel, M. Janssen, S. Samin, R. van Roij, Fundamental measure theory for the electric double layer: implications for blue-energy harvesting and water desalination, J. Phys.: Condens. Matter 27 (19) (2015) 194129.
- [10] D. Brogioli, Extracting renewable energy from a salinity difference using a capacitor, Phys. Rev. Lett. 103 (5) (2009) 058501.
- [11] R. Rica, R. Ziano, D. Salerno, F. Mantegazza, D. Brogioli, Thermodynamic relation between voltage-concentration dependence and salt adsorption in electrochemical cells, Phys. Rev. Lett. 109 (15) (2012) 156103.
- [12] M. Simoncelli, N. Ganfoud, A. Sene, M. Haefele, B. Daffos, P.-L. Taberna, M. Salanne, P. Simon, B. Rotenberg, Blue energy and desalination with nanoporous carbon electrodes: Capacitance from molecular simulations to continuous models, Phys. Rev. X 8 (2) (2018) 021024.
- [13] P. Biesheuvel, Y. Fu, M. Z. Bazant, Diffuse charge and Faradaic reactions in porous electrodes, Phys. Rev. E 83 (6) (2011) 061507.
- [14] A. Allagui, H. Alnaqbi, A. S. Elwakil, Z. Said, A. Hachicha, C. Wang, M. A. Abdelkareem, Fractional-order electric double-layer capacitors with tunable low-frequency impedance phase angle and energy storage capabilities, Appl. Phys. Lett. 116 (2020) 013902.
- [15] A. Allagui, T. J. Freeborn, A. S. Elwakil, B. J. Maundy, Reevaluation of Performance of Electric Double-layer Capacitors from Constant-current Charge/Discharge and Cyclic Voltammetry, Sci. Rep. 6 (38568).
- [16] A. Allagui, D. Zhang, A. S. Elwakil, Short-Term Memory in Electric Double-Layer Capacitors, Appl. Phys. Lett. 113 (2018) 253901–5.
- [17] A. Allagui, D. Zhang, I. Khakpour, A. S. Elwakil, C. Wang, Quantification of memory in fractional-order capacitors, J. Phys. D 53 (02LT03).
- [18] J.-P. Hansen, H. Löwen, Effective interactions between electric double layers, Annu. Rev. Phys. Chem. 51 (1) (2000) 209–242.
- [19] M. A. Brown, Z. Abbas, A. Kleibert, R. G. Green, A. Goel, S. May, T. M. Squires, Determination of surface potential and electrical double-layer structure at the aqueous electrolyte-nanoparticle interface, Phys. Rev. X 6 (1) (2016) 011007.
- [20] C. Outhwaite, Higher-order closures and potential problems in diffuse double layer and strong electrolyte solution theory, Mol. Phys. 27 (3) (1974) 561–575.
- [21] B. Uralcan, I. A. Aksay, P. G. Debenedetti, D. T. Limmer, Concentration fluctuations and capacitive response in dense ionic solutions, J. Phys. Chem. Lett. 7 (13) (2016) 2333–2338.

- [22] D. T. Limmer, C. Merlet, M. Salanne, D. Chandler, P. A. Madden, R. Van Roij, B. Rotenberg, Charge fluctuations in nanoscale capacitors, *Phys. Rev. Lett.* 111 (10) (2013) 106102.
- [23] A. Härtel, Structure of electric double layers in capacitive systems and to what extent (classical) density functional theory describes it, *J. Phys.: Condens. Matter* 29 (42) (2017) 423002.
- [24] K. B. Oldham, A Gouy–Chapman–Stern model of the double layer at a (metal)/(ionic liquid) interface, *J. Electroanal. Chem.* 613 (2) (2008) 131 – 138.
- [25] C. Gray, P. Stiles, Nonlinear electrostatics: the Poisson–Boltzmann equation, *Eur. J. Phys.* 39 (5) (2018) 053002.
- [26] B. Corry, S. Kuyucak, S.-H. Chung, Tests of continuum theories as models of ion channels. II. Poisson–Nernst–Planck theory versus Brownian dynamics, *Biophys. J.* 78 (5) (2000) 2364–2381.
- [27] A. G. Moreira, R. R. Netz, Strong-coupling theory for counter-ion distributions, *Europhys. Lett.* 52 (6) (2000) 705.
- [28] V. García-Morales, K. Krischer, Superstatistics in nanoscale electrochemical systems, *Proc. Natl. Acad. Sci.* 108 (49) (2011) 19535–19539.
- [29] C. Tsallis, Beyond Boltzmann–Gibbs–Shannon in Physics and Elsewhere, *Entropy* 21 (7) (2019) 696.
- [30] V. Garcia-Morales, J. Cervera, J. Pellicer, Coupling theory for counterion distributions based in Tsallis statistics, *Physica A* 339 (3) (2004) 482 – 490, ISSN 0378-4371.
- [31] C. Tsallis, Possible generalization of Boltzmann–Gibbs statistics, *J. Stat. Phys.* 52 (1-2) (1988) 479–487.
- [32] C. Beck, E. G. Cohen, Superstatistics, *Physica A* 322 (2003) 267–275.
- [33] C. Beck, Superstatistics: theory and applications, *Continuum Mech. Thermodyn.* 16 (3) (2004) 293–304.
- [34] S. Abe, C. Beck, E. G. Cohen, Superstatistics, thermodynamics, and fluctuations, *Phys. Rev. E* 76 (3) (2007) 031102.
- [35] M. Z. Bazant, M. S. Kilic, B. D. Storey, A. Ajdari, Towards an understanding of induced-charge electrokinetics at large applied voltages in concentrated solutions, *Adv. Colloid Interface Sci.* 152 (1-2) (2009) 48–88.
- [36] P. Biesheuvel, M. Van Soestbergen, Counterion volume effects in mixed electrical double layers, *J. Colloid Interface Sci.* 316 (2) (2007) 490–499.
- [37] A. A. Kornyshev, Double-layer in ionic liquids: paradigm change?, *J. Phys. Chem. B* 111 (20) (2007) 5545–5557.
- [38] B. A. Boukamp, A linear Kronig–Kramers transform test for immittance data validation, *J. Electrochem. Soc.* 142 (6) (1995) 1885–1894.
- [39] H. Hasegawa, Non-extensive thermodynamics of transition-metal nanoclusters, *Prog. Mater. Sci.* 52 (2-3) (2007) 333–351.
- [40] C. Tsallis, What should a statistical mechanics satisfy to reflect nature?, *Physica D* 193 (1-4) (2004) 3–34.
- [41] V. García-Morales, K. Krischer, Fluctuation enhanced electrochemical reaction rates at the nanoscale, *Proc. Natl. Acad. Sci.* 107 (10) (2010) 4528–4532.
- [42] N. Bonnet, T. Morishita, O. Sugino, M. Otani, First-principles molecular dynamics at a constant electrode potential, *Phys. Rev. Lett.* 109 (26) (2012) 266101.
- [43] M. Gell-Mann, C. Tsallis, *Nonextensive entropy: interdisciplinary applications*, Oxford University Press on Demand, 2004.
- [44] S. Abe, Y. Okamoto, *Nonextensive statistical mechanics and its applications*, vol. 560, Springer Science & Business Media, 2001.
- [45] R. Hanel, S. Thurner, M. Gell-Mann, Generalized entropies and the transformation group of superstatistics, *Proc. Natl. Acad. Sci.* 108 (16) (2011) 6390–6394.
- [46] C. Tsallis, Nonextensive statistics: theoretical, experimental and computational evidences and connections, *Braz. J. Phys.* 29 (1) (1999) 1–35.
- [47] E. P. Borges, On a q-generalization of circular and hyperbolic functions, *J. Phys. A: Math. Gen.* 31 (23) (1998) 5281.
- [48] A. Allagui, T. J. Freeborn, A. S. Elwakil, M. E. Fouda, B. J. Maundy, A. G. Radwanh, Z. Said, M. A. Abdelkareem, Review of Fractional-Order Electrical Characterization of Supercapacitors, *J. Power Sources* 400 (457–467).
- [49] M. E. Fouda, A. S. Elwakil, A. G. Radwan, A. Allagui, Power and Energy Analysis of Fractional-order Electrical Energy Storage Devices, *Energy* 111 (2016) 785–792.
- [50] D. Zhang, A. Allagui, A. S. Elwakil, A. M. Nassef, H. Rezk, J. Cheng, W. C. Choy, On the Modeling of Dispersive Transient Photocurrent Response of Organic Solar Cells, *Org. Electron.* 70 (2019) 42–47.

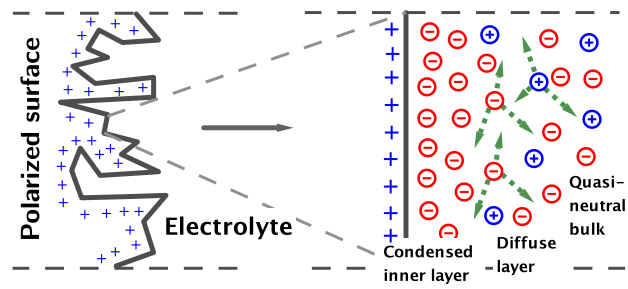


Figure 1: Schematic representation of electric double-layer structure at a positively-polarized blocking electrode/electrolyte interface. Its thickness (a measure of its capacity) is usually in the order of a few nanometers at most.

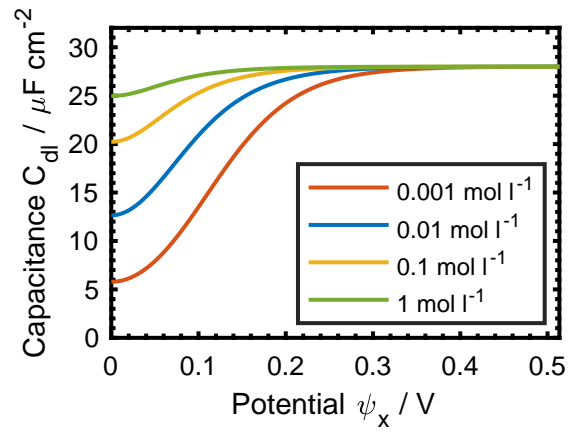


Figure 2: Plots of double-layer capacitance (Eq. 10) as a function of the potential across the double layer for different values of C_x^0 with $C_H = 28 \mu\text{F cm}^{-2}$, $\epsilon = 80 \epsilon_0$, $z = 1$, $T = 298 \text{ K}$

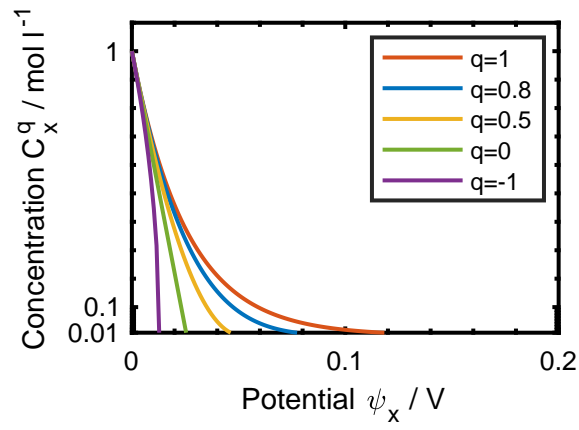


Figure 3: Plots of ion concentration (Eq. 14) as a function of the potential across the double layer for different values of q and with $C_x^0 = 1 \text{ mol l}^{-1}$, $z = 1$, $T = 298 \text{ K}$. The straight lines with the slope of $-zF/RT \ln(10)$ are for $q = 1.0$ only, otherwise the decay-plots follow power-law profiles.

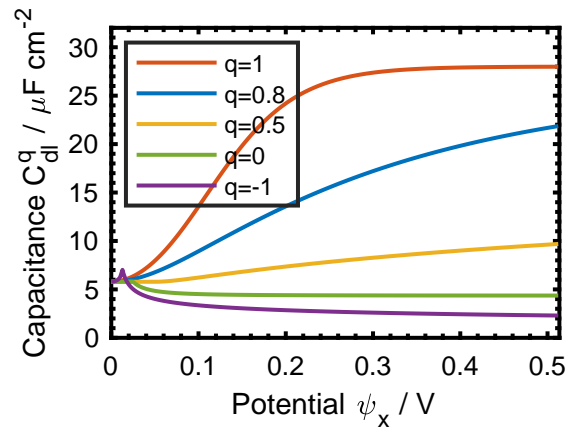


Figure 4: Plots of double-layer capacitance (Eq. 23) as a function of the potential across the double layer for different values of q (from -1 to 1) with $C_x^0 = 10^{-3} \text{ mol l}^{-1}$, $C_H = 28 \mu\text{F cm}^{-2}$, $\epsilon = 80 \epsilon_0$, $z = 1$ and $T = 298 \text{ K}$